Ninth International Conference on
THIN-WALLED STRUCTURES – ICTWS2023
Sydney, Australia, Nov 29 – Dec 1, 2023

THE EFFECT OF ROOF CURVATURE ON THE RIGIDITY AND STABILITY OF CABLE DOMES

Elshaimaa A. Ahmed* and Ashraf A. El Damatty**

* The University of Western Ontario, London, Canada

Mansoura University, Mansoura Egypt
e-mail: eahmed23@uwo.ca

** The University of Western Ontario, London, Canada
e-mail: damatty@uwo.ca

Keywords: Cable domes; Buckling; Rigidity; Structural optimization; Zero-Gaussian curvature; Negative-Gaussian curvature.

Abstract. *The aesthetic view and versatile forms of cable domes attracted many designers to develop new forms with better stability and rigidity. The roof curvature has crucial effect on the rigidity, stability, and optimum weight of cable domes at specific target displacement. This study considers four cases of cable domes of Geiger type: a positive-, zero, and two negative-Gaussian curvature cable domes. The four case studies have the same cable-struts arrangement and dimensions in plan, the same length of struts and mid-point height above the lowest point in the roof. Form-finding is performed first for the four cases to obtain a feasible geometry with a feasible set of prestresses. An optimization of prestress level and size of elements is then performed with the aim of minimizing structural weight under external uniform load of 1.0 kN/m^2 at target displacement L/500 with constraints on the stability of struts and strength of cables. The rigidity and stability of the optimized forms are eventually investigated and compared by increasing the external loads from 0.0 to 10.0 kN/m^2 using Arc-Length method. The comparison shows that negative-Gaussian curvature cable domes have better stability and rigidity than the corresponding zero- and positive-Gaussian curvature domes.*

1 INTRODUCTION

Cable domes are considered as hybrid tensile structures that exploit the self-stability of prestressed tensegrity structures composed mainly of cables and struts, but with marginal beams. The light weight, aesthetic appearance, and flexibility in designing cable domes motived designers to develop new forms of cable domes with more stability and rigidity. The first step in developing a new form of cable domes is to propose a desirable configuration, then, finding a geometrical shape that leads to a feasible set of prestress through a process called form-finding [1]. Previous research [1-8] addressed the problem of form-finding of pin-jointed structures in general and cable domes in particular. The feasible set of prestresses resulting from the form-finding process is not unique and can be modified according to the mechanical properties and load carrying capacity of the dome. Different levels of prestress lead, in turn, to different levels of structural stiffness. Therefore, in practical applications, form-finding should be followed by structural optimization taking into consideration additional design parameters such as rigidity, deformations, stability, stress intensity and/or structural weight. Various studies [9-14] addressed this topic in the literature. Other studies [15-18] addressed the shape optimization of tensegrity structures under buckling or compliance constraints aiming at maximizing the stiffness of the structure or minimizing the structural weight.

The main problem in traditional forms of cable domes with positive curvature is the potential instability under excessive loading due to slacking in cables and/or buckling in struts. The

newly developed negative-Gaussian curvature cable domes, however, are intended to have better stability and rigidity than the positive ones due to the double curvature of the roof; the positive curve has the supporting (*bearing*) function while the negative one has a *stabilizing* function. Moreover, the rigidity and stability of cable domes are highly affected by the rise and sag values of the positive and negative curves comprising the saddle-shape surface. In this regard, this study considers four cases of cable domes of Geiger type: a positive-, zero-, and two negative-Gaussian curvature cable domes. The four case studies have the same cable-struts arrangement and dimensions in plan, length of struts, and mid-point height above the lowest point in the roof. The positive-curvature dome surface is developed by rotating one positive curve around the vertical axis. Zero- and negative-curvature domes are developed by translating a positive curve over a straight line and a negative curve, respectively. All cases have the same rise value of the positive curve. For the negative-curvature domes, two sag values of the negative curve are considered to study the effect of the rise/sag value on the stability and rigidity of the dome.

Form-finding is performed first for the four cases to obtain a feasible geometry with a feasible set of prestresses. In the current study, the NURBS-based form-finding algorithm [19], developed recently by the authors of the current paper, is employed in order to develop a feasible form with predefined rise and sag values. The algorithm controls the dome curvature using NURBS curves through a Genetic Algorithm (GA) that aims at finding a feasible form while maintaining the required rise and sag values. The variables of the algorithm are the locations and weights of the control points of two NURBS curves forming the dome's outer surface. Distinguishably from other form-finding methods available in the literature, this algorithm can be applied on cable domes with either zero-, positive-, or negative-Gaussian curvature, serving as a crucial tool in studying the effect of roof curvature on the rigidity and stability of such forms.

The four cases are then designed to have the same stiffness and weight using the Incremental-Prestressing (IP) Iterative Technique developed by Ahmed et al. [14]. The variables of this technique are the prestress level and size of elements; It aims to minimize the structural weight under external uniform load of 1.0 kN/m^2 at target displacement L/500 with constraints on the stability of struts and strength of cables. The rigidity and stability of the optimized forms are eventually investigated and compared by increasing the external loads from 0.0 to 10.0 kN/m^2 using Arc-Length method. The rigidity of domes is assessed based on the maximum vertical displacement reached at the last load step while their stability is assessed based on buckling of struts and slacking or yielding of cables during the calculations. The comparison shows that negative-Gaussian curvature cable domes have better stability and rigidity than the corresponding zero- and positive-Gaussian curvature domes.

This paper is organized as follows. Section 2 demonstrates the form-finding and optimization techniques used to design the case studies of cable domes and their results. Section 3 provides the results of the Arc-Length method, compares, and discusses the stability and rigidity of four cases of roof curvature. Section 4 concludes the results.

2 METHODOLOGY

2.1 Form-finding

As indicated in the previous section, four cases of cable domes with different roof curvatures are developed and optimized to the minimum weight at displacement constraint L/500 under uniform vertical load 1.0 kN/m^2 in order to compare their rigidity and stability when increasing the vertical loads from 0.0 to 10.0 kN/m^2. The positive-curvature (PC) dome is developed by rotating a positive curve with a rise of 16 m around *z* axis as shown in Figure 1 (a). The zero-

curvature (ZC) dome is developed by translating a positive curve with rise 16 m over a straight line whereas the negative-curvature (NC) dome is developed by translating a positive curve with rise 16 m over a negative one with sag 8 m and 16 m as shown in Figure 1 (b-c). The rise of all cases is set to 16 m. The arrangement of cables and struts, x and y coordinates of all nodes, and length of struts are identical as shown in Figure 2. *z* coordinates and the associated feasible prestress are unknown and can be determined using the NURBS-based form-finding algorithm developed by Ahmed et al. [19]. The algorithm employs four control points to represent each of positive and negative curves comprising the dome surface. The location and weight of control points are the variables of a GA algorithm which aims at finding a feasible form that fulfills the feasibility conditions: 1) symmetry, 2) unilateral, 3) equilibrium, and 4) stability. The prestress is calculated at each iteration using Singular-Value Decomposition (SVD) technique developed by Pellegrino [20]. More details on the form-finding algorithm can be found in [19]. The feasible geometry and associated feasible prestress at the end of the form-finding for the four cases are presented in Table 1 to Table 3.

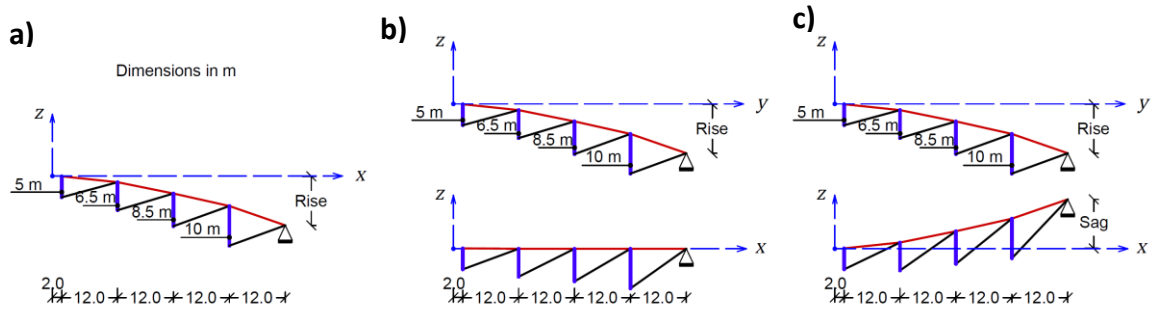

Figure 1: Illustration of rise and sag of the outer surface of a) positive, b) zero, and c) negative curvature domes.

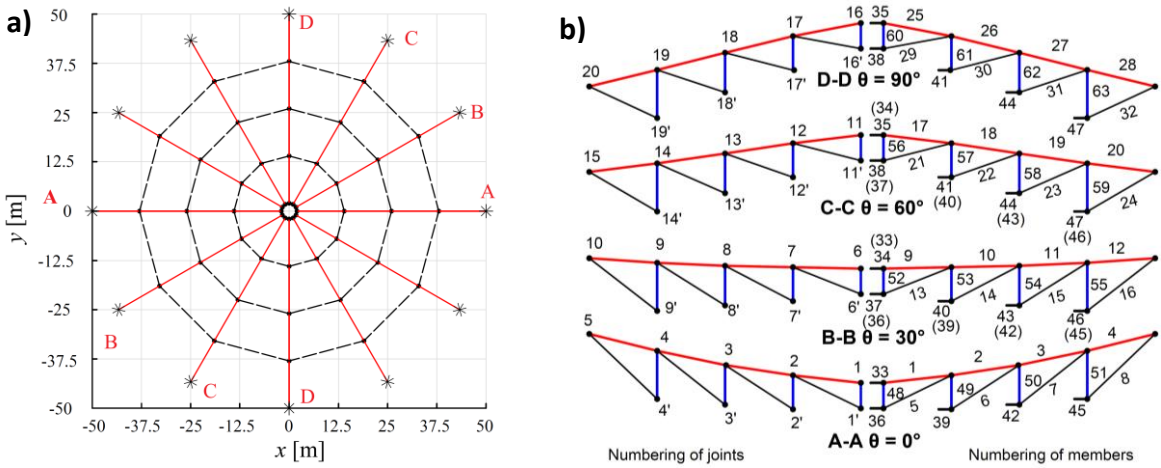

Figure 2: a) Plan view of case studies of cable domes, and b) numbering of joints and members.

Table 1: Vertical coordinates of the upper nodes at the end of form-finding algorithm and base prestress **f** [unitless] scaled to member No. 33 for case 1 (PC dome).

Node		***z* [m]**	**Mem. #**	**Prestress**	**Mem. #**	**Prestress**	**Mem. #**	**Prestress**	**Mem. #**	**Prestress**
	1	-0.059	1	0.5176	6	0.2368	39	0.4060	50	-0.1048
	2	-1.661	2	0.6005	7	0.3698	42	0.5872	51	-0.2055
A-A	3	-4.809	3	0.8101	8	0.7389	45	1.1037		
	4	-9.322	4	1.1127	**33**	**1.0000**	48	-0.0298		
	5	**-16.000**	5	0.0904	36	0.1601	49	-0.0560		

Table 2: Vertical coordinates of the upper nodes at the end of form-finding for case 2 (ZC dome), 3 (NC dome with sag 4 m), and 4 (NC dome with sag 8 m).

Node		*z* [m] for case			Node		*z* [m] for case		
		2	**3**	**4**			**2**	**3**	**4**
	1	0.023	0.035	0.045		11	-0.039	-0.045	-0.063
	2	0.250	0.276	0.750		12	-1.185	-1.630	-1.846
A-A	3	0.048	0.547	1.953	C-C	13	-3.599	-4.494	-4.645
	4	-0.024	1.729	4.242		14	-7.004	-7.911	-8.084
	5	**0.000**	**4.000**	**8.000**		15	-12.001	-12.035	-11.477
	6	0.002	0.008	0.007		16	-0.059	-0.071	-0.098
	7	-0.234	-0.407	-0.214		17	-1.661	-2.208	-2.602
B-B	8	-1.192	-1.358	-0.662	D-D	18	-4.809	-5.935	-6.430
	9	-2.431	-2.139	-1.006		19	-9.322	-10.487	-11.159
	10	-4.235	-2.896	-0.832		20	**-16.000**	**-16.000**	**-16.000**

Table 3: Base prestress f [unitless] for case 2 (ZC dome), 3 (NC dome with sag 4 m), and 4 (NC dome with sag 8 m) scaled to member No. 33.

Mem. #	Prestress for case			Mem. #	Prestress for case			Mem. #	Prestress for case		
	2	**3**	**4**		**2**	**3**	**4**		**2**	**3**	**4**
1	0.5176	0.5176	0.5183	22	0.2215	0.2673	0.2050	43	0.5940	0.5352	0.4116
2	0.6005	0.6442	0.6447	23	0.3288	0.2930	0.2218	44	0.5870	0.5242	0.3982
3	0.8101	0.9042	0.8525	24	0.6144	0.3604	0.1705	45	1.1037	0.6374	0.2986
4	1.1127	1.1904	1.0915	25	0.5221	0.5256	0.5285	46	1.1248	0.6518	0.3066
5	0.0904	0.1381	0.1375	26	0.6207	0.6744	0.6734	47	1.1031	0.6307	0.2920
6	0.2368	0.2937	0.2327	27	0.8654	0.9624	0.9000	48	-0.0298	-0.0424	-0.0417
7	0.3698	0.3467	0.2748	28	1.2734	1.2872	1.1232	49	-0.0560	-0.0512	-0.0251
8	0.7389	0.4630	0.2272	29	0.0861	0.1301	0.1268	50	-0.1048	-0.0702	-0.0303
9	0.5176	0.5178	0.5174	30	0.2177	0.2626	0.2007	51	-0.2055	-0.0851	-0.0173
10	0.6023	0.6460	0.6419	31	0.3189	0.2840	0.2142	52	-0.0298	-0.0424	-0.0417
11	0.8144	0.9018	0.8377	32	0.5884	0.3456	0.1625	53	-0.0707	-0.0815	-0.0639
12	1.1252	1.1720	1.0418	**33**	**1.0000**	**1.0000**	**1.0000**	54	-0.1325	-0.1258	-0.0988
13	0.0891	0.1355	0.1336	34	1.0006	1.0010	1.0018	55	-0.2668	-0.1888	-0.0998
14	0.2310	0.2819	0.2194	35	1.0000	1.0000	1.0000	56	-0.0298	-0.0424	-0.0417
15	0.3538	0.3208	0.2470	36	0.1601	0.2446	0.2400	57	-0.0979	-0.1214	-0.1061
16	0.6868	0.4086	0.1958	37	0.1602	0.2448	0.2404	58	-0.1805	-0.1800	-0.1506
17	0.5199	0.5220	0.5230	38	0.1601	0.2445	0.2399	59	-0.3620	-0.2601	-0.1409
18	0.6124	0.6621	0.6587	39	0.4060	0.4964	0.3817	60	-0.0298	-0.0424	-0.0417
19	0.8420	0.9356	0.8710	40	0.4086	0.5012	0.3878	61	-0.1118	-0.1380	-0.1225
20	1.2053	1.2368	1.0825	41	0.4060	0.4958	0.3804	62	-0.2057	-0.2004	-0.1689
21	0.0870	0.1316	0.1285	42	0.5872	0.5264	0.4021	63	-0.4152	-0.2848	-0.1544

2.2 Prestress and size optimization

Following the form-finding, a structural optimization is performed to the cross-sectional areas of all elements and base prestress multiplier γ of the feasible form developed at the end of form-finding algorithm under uniform external loads 1.0 kN/m^2. This study adopts the IP iterative technique proposed by Ahmed et al. [21] because of its time-efficiency and robustness in minimizing the total weight of cable domes with constraints on the stability and strength of elements. The material properties and list of cross-sectional areas are provided in Table 4 for cables and struts. The optimization algorithm depends on prestressing the dome with an initial value of prestress level that ensures starting from a feasible state, i.e., with no slack in cables. Then, the prestress level is increased incrementally until reaching maximum displacement less than L/500 (0.2 m), where L is the dome diameter. At each increment, the dome is optimized to the minimum weight that fulfills the following constraints: 1) no yielding in cables, and 2) no buckling in struts as presented in Eq. (1) and Eq. (2), respectively, according to CAN/CSA S16-

14 [22] where $\varphi = 0.9$, $n = 1.34$, A_c and A_s is the area of cables and struts, respectively. F_c and F_s are the normal forces in cables and struts, respectively. σ_c is the yield strength of cables, σ_s is the yield strength of struts, ξ is a factor of safety equal to 0.3 in the current study, and λ can be calculated using Eq. (3), where $K = 1.0$, L is the strut's length, and r is the radius of gyration of cross section. A relaxation factor of ($R_e = 0.95$) is also used to prevent divergence.

$$F_c \leq \xi \varphi A_c \sigma_c \tag{1}$$

$$F_s \leq \frac{\xi \varphi A_s \sigma_s}{(1+\lambda^{2n})^{\frac{1}{n}}} \tag{2}$$

$$\lambda = \frac{KL}{r}\sqrt{\frac{\sigma_s}{\pi^2 E_s}} \tag{3}$$

The results of optimized weight W_T in [N] and the corresponding prestress level γ in [N] at the end of optimization algorithm (at $\delta \leq 0.2$ m) are presented in Table 5. It has been noticed that PC dome requires a larger prestress level than the corresponding ZC and NC domes. Level of prestress required for PC dome to sustain 1.0 kN/m^2 external loads at displacement of order 0.2 m is approximately 88 MN whereas 10, 13, and 18 MN prestress levels are required for ZC and NC domes with sag 4 m and 8 m, respectively, to sustain the same external loads and at the same displacement (stiffness) values. This can be attributed to the ability of the stabilizing cables in ZC and NC domes in supporting the bearing cables to sustain the external loads. The total weight, however, increases slightly from 2.7 to 3.3 MN when increasing the sag value from 0 to 8 m. The PC dome weight is the least among all cases with approximately 2.5 MN. The optimized cross sections' dimensions including the outer diameter and thickness of hollow round sections of struts and diameter of cables are presented in Table 6 and Table 7.

Table 4: Properties of cross sections used in the numerical optimization.

	Struts	**Cables**
Grade of steel:	ASTM A500 Grade C	ASTM A416 Grade 270
Yield strength:	$\sigma_s = 317$ MPa	$\sigma_c = 1670$ MPa
Modulus of elasticity:	$E_s = 2.06 \times 10^5$ MPa	$E_c = 1.965 \times 10^5$ MPa
Section:	Hollow Round: $D_s = 0.020, 0.024, \ldots.$ (m) $t_s = D_s/40$	Circular: $D_c = 0.020, 0.022, \ldots.$ (m)

Table 5: The optimized results of displacement, structural weight, and prestress level for all cases.

	Case 1 PC Dome	**Case 2 ZC Dome**	**Case 3 NC Dome – Sag 4 m**	**Case 4 NC Dome – Sag 8 m**
δ [m]	0.182	0.187	0.195	0.197
W_T [N]	2,472,100	2,746,800	3,119,600	3,306,000
γ [N]	88,539,000	10,000,000	13,000,000	18,000,000

Table 6: Thickness of HSS of struts [m] in all cases.

Mem. #	**Case**	**Mem. #**	**Case**			**Mem. #**	**Case**		
	1		**2**	**3**	**4**		**2**	**3**	**4**
48	0.0040	48	0.0061	0.0079	0.0092	56	0.0061	0.0077	0.0089
49	0.0067	49	0.0087	0.0094	0.0083	57	0.0105	0.0129	0.0142
50	0.0111	50	0.0121	0.0116	0.0097	58	0.0147	0.0165	0.0176
51	0.0188	51	0.0168	0.0136	0.0094	59	0.0209	0.0205	0.0185
		52	0.0060	0.0077	0.0088	60	0.0061	0.0078	0.0089
		53	0.0093	0.0109	0.0114	61	0.0112	0.0138	0.0152
		54	0.0131	0.0143	0.0148	62	0.0156	0.0174	0.0186
		55	0.0185	0.0180	0.0161	63	0.0222	0.0214	0.0193

Table 7: Diameter [m] in all cases.

Mem. #	Case	Mem. #	Case			Mem. #	Case			Mem. #	Case		
	1		2	3	4		2	3	4		2	3	4
1	0.040	1	0.116	0.140	0.172	22	0.084	0.104	0.108	43	0.140	0.152	0.156
2	0.128	2	0.128	0.156	0.192	23	0.104	0.112	0.116	44	0.140	0.152	0.152
3	0.148	3	0.148	0.188	0.220	24	0.144	0.128	0.108	45	0.196	0.172	0.144
4	0.180	4	0.180	0.216	0.248	25	0.116	0.136	0.164	46	0.196	0.172	0.144
5	0.052	5	0.052	0.072	0.088	26	0.128	0.156	0.184	47	0.196	0.172	0.140
6	0.084	6	0.084	0.108	0.116	27	0.152	0.188	0.216	48	0.244	0.316	0.368
7	0.112	7	0.112	0.124	0.128	28	0.192	0.220	0.244	49	0.348	0.376	0.332
8	0.160	8	0.160	0.148	0.128	29	0.052	0.072	0.080	50	0.484	0.464	0.388
33	0.160	9	0.112	0.132	0.160	30	0.084	0.104	0.104	51	0.672	0.544	0.376
36	0.068	10	0.124	0.148	0.176	31	0.104	0.112	0.112	52	0.240	0.308	0.352
39	0.112	11	0.148	0.180	0.204	32	0.144	0.128	0.104	53	0.372	0.436	0.456
42	0.140	12	0.176	0.208	0.232	33	0.160	0.184	0.224	54	0.524	0.572	0.592
45	0.196	13	0.052	0.072	0.084	34	0.160	0.188	0.224	55	0.740	0.720	0.644
48	0.244	14	0.084	0.104	0.108	35	0.160	0.188	0.224	56	0.244	0.308	0.356
49	0.348	15	0.108	0.116	0.120	36	0.068	0.096	0.112	57	0.420	0.516	0.568
50	0.484	16	0.156	0.140	0.116	37	0.068	0.096	0.112	58	0.588	0.660	0.704
51	0.672	17	0.116	0.132	0.160	38	0.068	0.096	0.112	59	0.836	0.820	0.740
		18	0.124	0.152	0.180	39	0.112	0.140	0.144	60	0.244	0.312	0.356
		19	0.148	0.184	0.208	40	0.112	0.140	0.144	61	0.448	0.552	0.608
		20	0.184	0.216	0.236	41	0.112	0.140	0.144	62	0.624	0.696	0.744
		21	0.052	0.072	0.080	42	0.140	0.152	0.156	63	0.888	0.856	0.772

3 RESULTS AND DISCUSSION

Domes' rigidity and stability are compared by increasing the external loads using Arc-Length method in ANSYS [23] software through SHARCNET high performance computing (HPC). The optimized weight and prestress level provided in Table 5 are applied in all case studies of cable domes at the first load step (at load multiplier = 0) whereas the external loads are increased incrementally from 0 to 10 (× 1.0 kN/m^2) using the Arc-Length method. The Arc-Length method [24] is an efficient method in solving non-linear systems of equations when the problem being solved exhibits one or more critical points and the model experiences instability when increasing the external forces. The bearing capacity of cable domes to sustain excessive loading is defined by the following limit states, namely: 1) strut buckling, 2) serviceability, and 3) cable rupture. Practice reveals that strut buckling and excessive deformation beyond the serviceability limit of *L*/250 occur within the elastic range of the material whereas cable rupture occurs in the inelastic range after the yield limit [25]. In the current study, the rigidity of domes is assessed based on the maximum vertical displacement reached at the last load step while the stability is assessed based on buckling of struts and slacking or yielding of cables during the calculations.

3.1 Rigidity

The results of maximum total deformation with the external load multiplier for four case studies (PC, ZC, NC dome with sag = 4 and 8 m) are presented in Figure 3. 3-D view of the deformed shapes at the last load step (at 10.0 kN/m^2) is shown in Figure 4. It can be noticed that the stiffness of PC dome decreases rapidly and the dome experiences large displacement at load multiplier 2.25 due to slack in ridge cables connected to the inner ring as shown in Figure 4 (a). The maximum deformation reached at the last load step is 7.34 m which violates the serviceability limit state of *L*/250 (0.4 m). The slacking cables of PC dome at the last load step are highlighted in Figure 6 (a).

On the other hand, none of the ZC and NC domes experience slack in cables throughout the calculations. However, the stiffness of ZC dome decreases at load multiplier 6.15 due to the rotation of the upper nodes of struts to reach 2.22 m maximum deformation at the last load step as shown in Figure 4 (b). The NC domes have shown more rigidity than the ZC and PC domes. The rigidity/stiffness of NC domes increases slightly when increasing sag of negative curve. The max deformation reached at the last load step for NC domes is approximately 1.2 m.

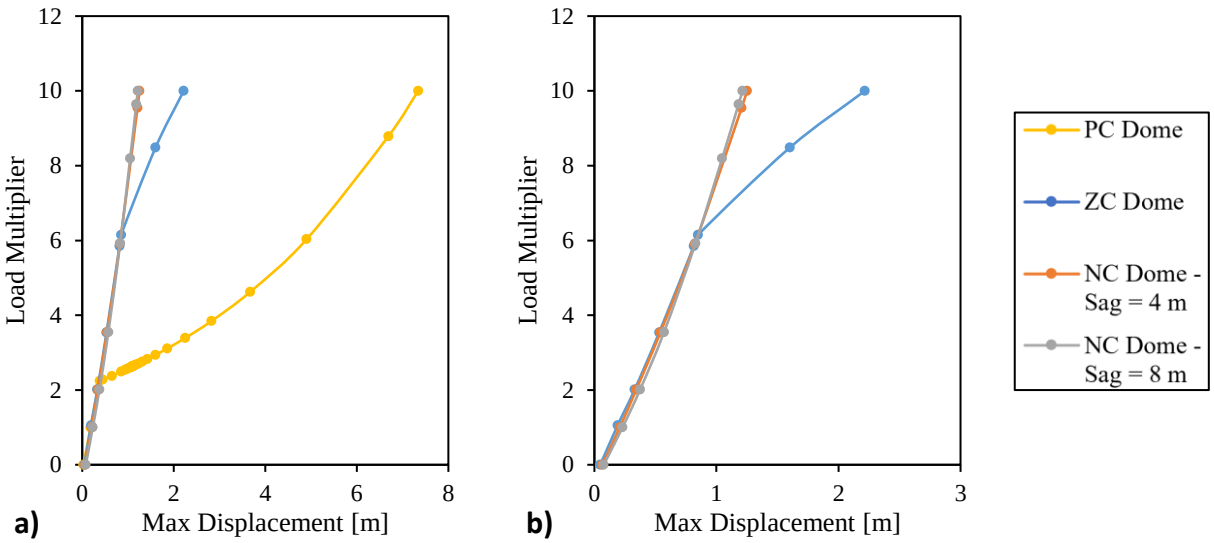

Figure 3: Maximum total deformation at all load steps using Arc-Length method for a) all cases, and b) ZC and NC domes only.

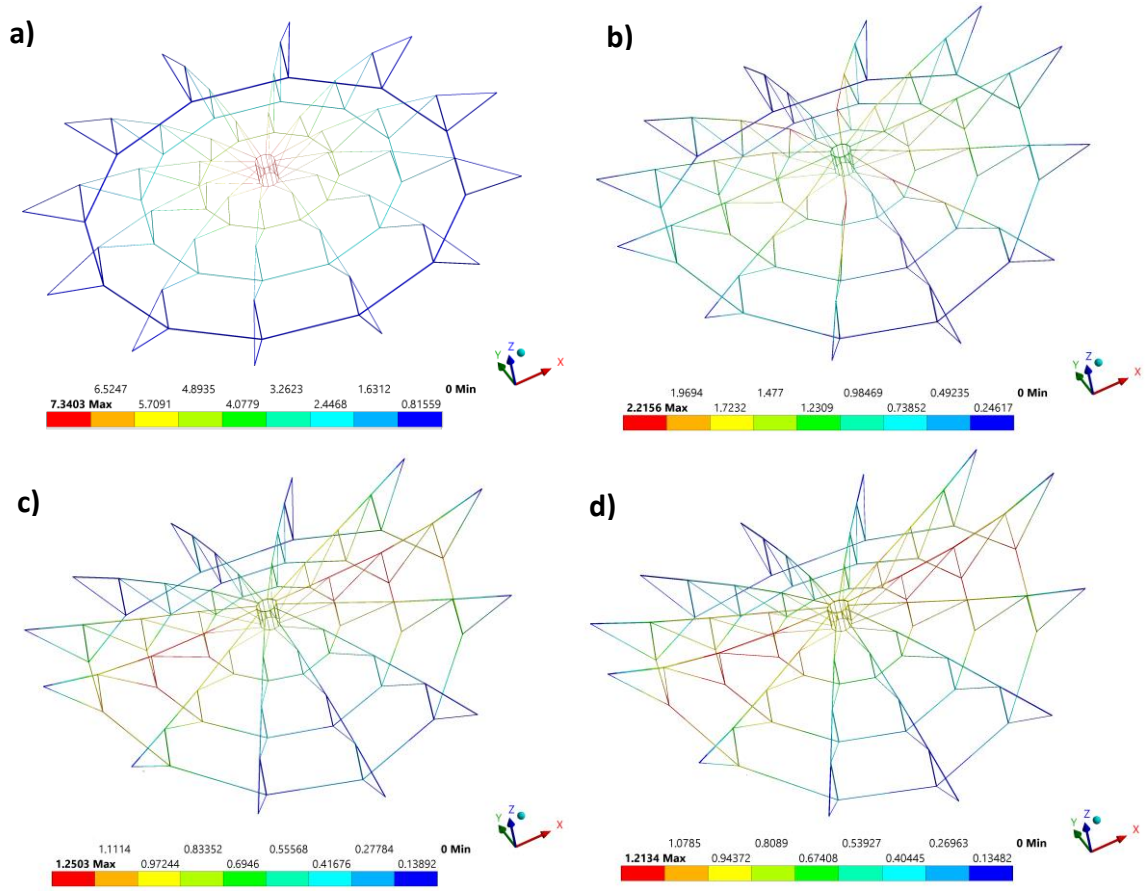

Figure 4: 3-D view of the deformed shape of a) PC, b) ZC, c) NC dome with sag = 4 m, and d) NC dome with sag = 8 m at the last load step (10.0 kN/m^2).

3.1 Stability

The results of maximum and minimum stresses in cables and struts for four domes with the load multiplier are presented in Figure 5. Buckling occurs when the normal stresses in struts F_s violate the condition of compressive strength provided in Eq. (4). For the PC dome, the maximum tensile stress in cables increases to 1.16 GPa at the last load step before the yielding limit of the material. Slack in cables represented by zero minimum stresses occurs in PC dome at 2.25 load multiplier whereas buckling in all struts occurs at 8.8 load multiplier except for the inner ring struts, around which slack occurred as shown in Figure 6 (b).

$$F_s \leq \frac{\varphi A_s \sigma_s}{(1+\lambda^{2n})^{\frac{1}{n}}} \tag{4}$$

The maximum tensile stresses in cables reached at the last load step for ZC and NC domes with sag 4 and 8 m are 0.95, 0.97, and 1.06 GPa, respectively, all of which are below the yield limit of the material. No buckling in struts occurs in ZC dome despite its kinematic instability discussed in the previous subsection. The NC domes with sag 4 and 8 m, however, experience slack in the outermost struts highlighted in Figure 6 (c-d) and located on the stabilizing cables at load multiplier 9.55 and 5.93, respectively. This indicates that increasing the sag of stabilizing cables decreases the stability of NC domes. It should be noted no slack in cables occurs in ZC and NC domes. The above results reveal that negative-Gaussian curvature cable domes have better stability and rigidity than the corresponding zero- and positive-Gaussian curvature domes.

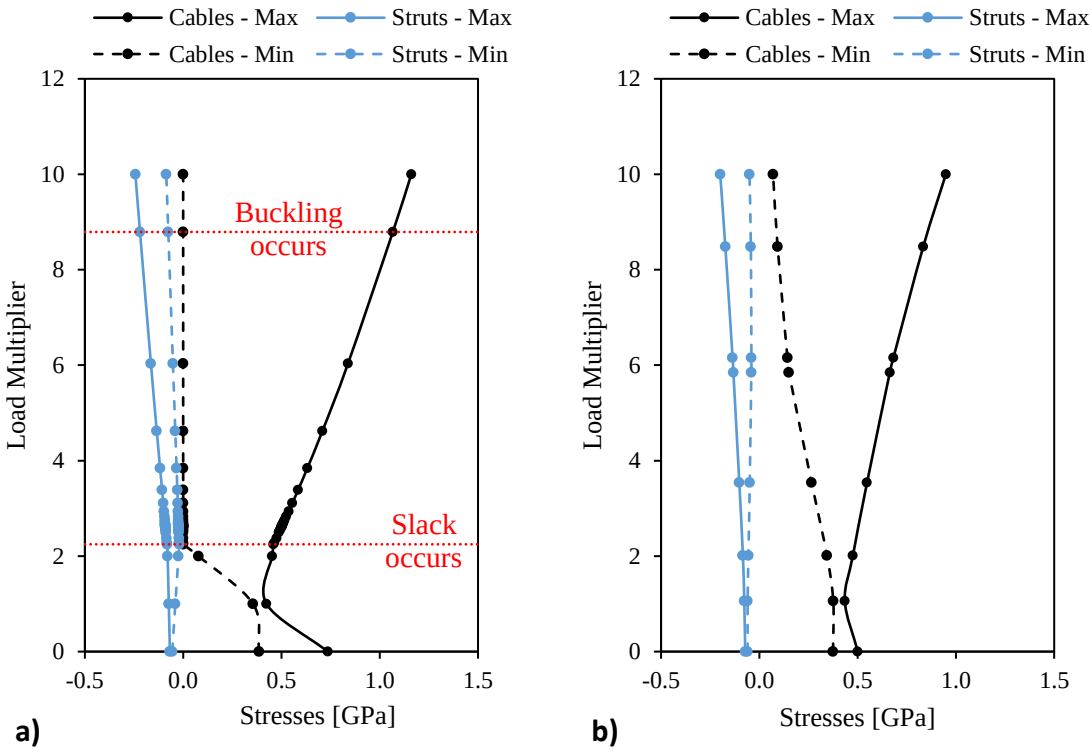

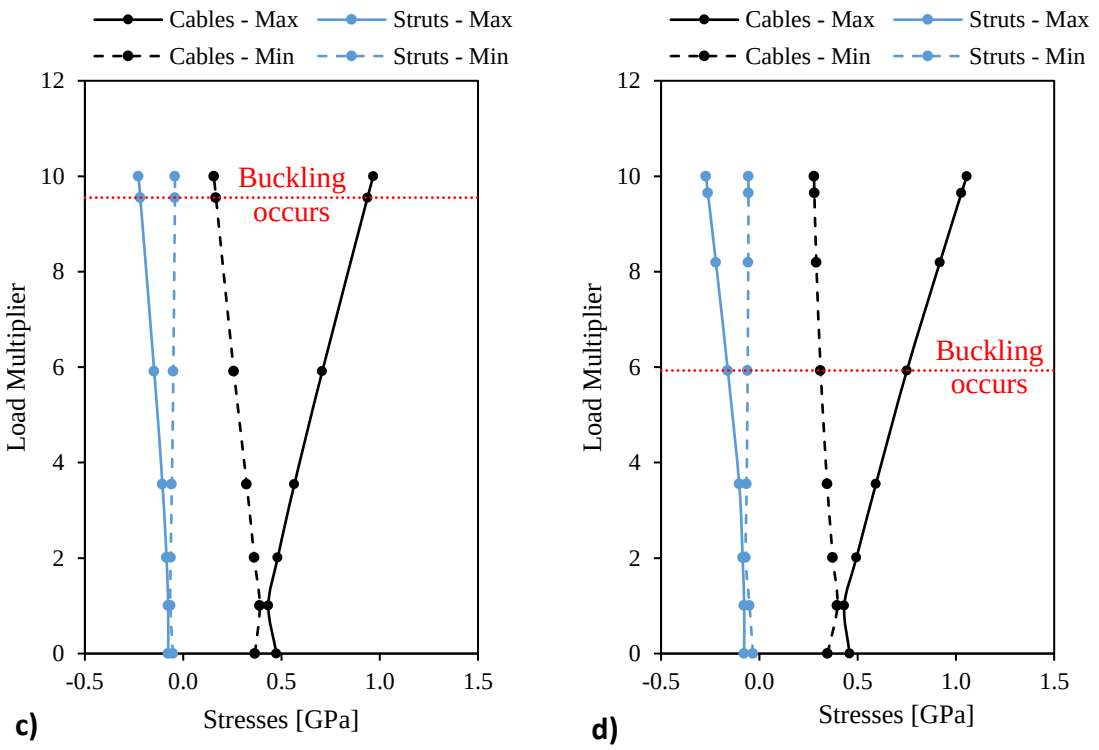

Figure 5: maximum (dotted line) and minimum (solid line) stresses in cables (in black) and struts (in blue) with the external load multiplier for of a) PC, b) ZC, c) NC dome with sag = 4 m, and d) NC dome with sag = 8 m.

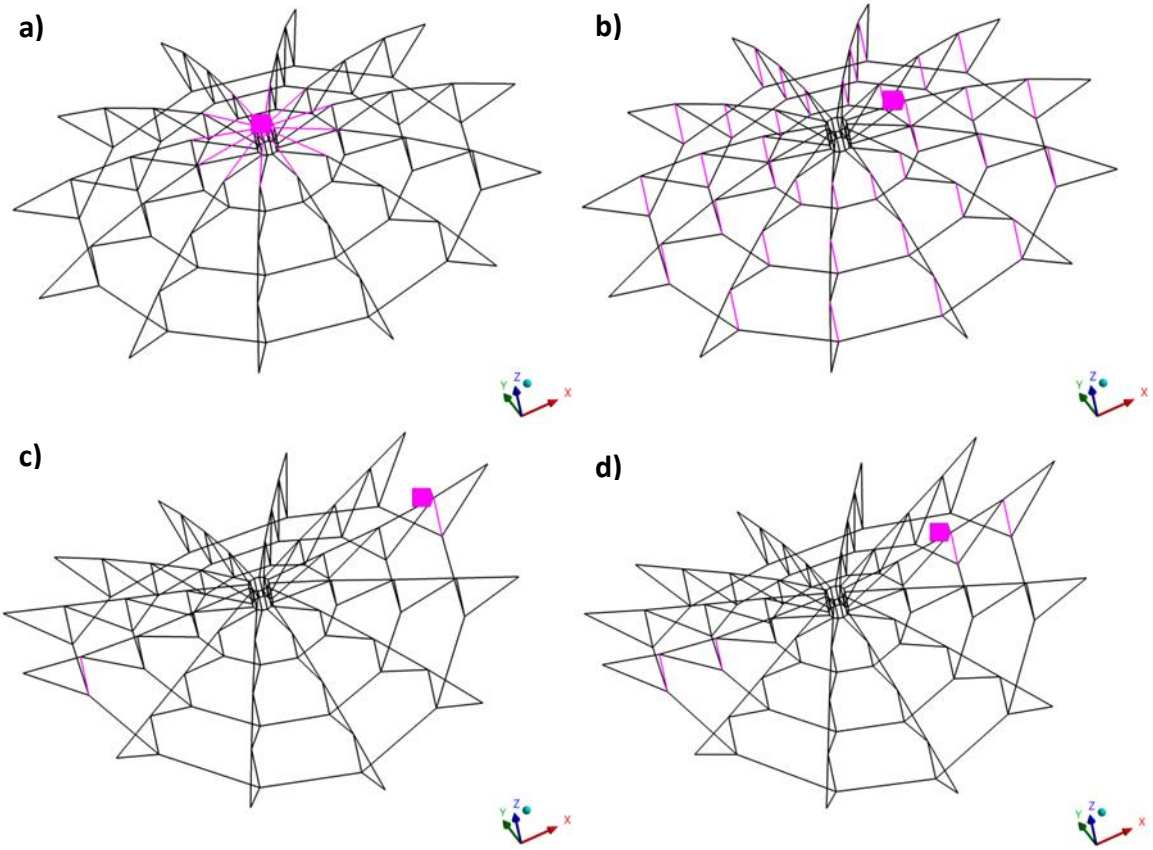

Figure 6: Highlights (in rose) of the elements experience a) slack and b) buckling in PC dome, and buckled struts in NC domes with sag c) 4 m and d) 8 m at the last load step.

4 CONCLUSIONS

To conclude, this study discusses and compares the rigidity and stability of four case studies of cable domes with different roof curvature: positive-, zero-, and two negative-curvature cable domes with sag 4 and 8 m. The domes are designed and optimized under external loading 1.0 kN/m^2 with a factor of safety of 30% of the allowable compressive and tensile stresses. The maximum vertical displacement in all cases is kept at 0.2 m to compare the optimized domes at the same stiffness values. The external loads are then increased incrementally to 10.0 kN/m^2 using Arc-Length method and the total deformation and stresses in all elements are monitored and compared for all cases. The rigidity of domes is assessed based on the maximum vertical displacement reached at the last load step while the stability is assessed based on buckling of struts and slack or yielding of cables during the calculations. The following remarks are concluded:

1) Positive-curvature dome loses its stability and rigidity rapidly due to slacking in the ridge cables around the inner ring and buckling in all struts when increasing external loads.
2) Zero-curvature dome has better stability and rigidity than the positive-curvature one. It does not experience slacking nor buckling. However, it loses its rigidity at higher values of external loads due to the kinematic instability of some of the upper nodes of struts.
3) Negative-curvature domes are more rigid and stable than zero- and positive-curvature domes. They do not experience slacking in cables and their rigidity increases when increasing the external loads. Buckling, however, occurs in a few numbers of outermost struts along the stabilizing cables. Stability increases when decreasing sag value in NC domes.

REFERENCES

[1] A. Tibert and S. Pellegrino, "Review of form-finding methods for tensegrity structures," International Journal of Space Structures, vol. 18, no. 4, pp. 209-223, 2003.

[2] J. Zhang and M. Ohsaki, "Adaptive force density method for form-finding problem of tensegrity structures," International Journal of Solids and Structures, vol. 43, no. 18-19, pp. 5658-5673, 2006.

[3] L. Zhang, B. Maurin, and R. Motro, "Form-finding of nonregular tensegrity systems," Journal of Structural Engineering, vol. 132, no. 9, pp. 1435-1440, 2006.

[4] H. C. Tran and J. Lee, "Form-finding of tensegrity structures using double singular value decomposition," Engineering with Computers, vol. 29, no. 1, pp. 71-86, 2013.

[5] Y. Wang, X. Xu, and Y. Luo, "Form-finding of tensegrity structures via rank minimization of force density matrix," Engineering Structures, vol. 227, p. 111419, 2021.

[6] Y. Xue, Y. Luo, and X. Xu, "Form-finding of cable-strut structures with given cable forces and strut lengths," Mechanics Research Communications, vol. 106, p. 103530, 2020.

[7] H. C. Tran and J. Lee, "Advanced form-finding for cable-strut structures," International Journal of Solids and Structures, vol. 47, no. 14-15, pp. 1785-1794, 2010.

[8] J. Guo and J. Jiang, "An algorithm for calculating the feasible pre-stress of cable-struts structure," Engineering Structures, vol. 118, pp. 228-239, 2016.

[9] F. Biondini, P. G. Malerba, and M. Quagliaroli, "Structural optimization of cable systems by genetic algorithms," in Proceedings of the 2011 world congress on advances in structural engineering and mechanics. Korea: Seoul, 2011.

[10] M. Quagliaroli, P. G. Malerba, A. Albertin, and N. Pollini, "The role of prestress and its optimization in cable domes design," Computers & Structures, vol. 161, pp. 17-30, 2015.

[11] A. Kaveh and M. Ilchi Ghazaan, "Optimal design of dome truss structures with dynamic frequency constraints," Structural and Multidisciplinary Optimization, vol. 53, no. 3, pp. 605-621, 2016.

[12] N. Pollini, "Gradient-based prestress and size optimization for the design of cable domes," International Journal of Solids and Structures, vol. 222, p. 111028, 2021.

[13] L. Chen, Y. Zeng, W. Gao, Y. Liu, and Y. Zhou, "Section Optimization Design of a Flexible Cable-Bar Tensile Structure Based on Robustness," Applied Sciences, vol. 11, no. 19, p. 8816, 2021.

[14] E. A. Ahmed, A. O. Nassef, and A. A. El Damatty, "Prestress and size optimization of double-curvature cable domes using an incremental-prestressing iterative technique," Thin-Walled Structures Journal, vol. 186, p. 110655, 2023.

[15] M. Kawaguchi, I. Tatemichi, and P. S. Chen, "Optimum shapes of a cable dome structure," Engineering Structures, vol. 21, no. 8, pp. 719-725, 1999.

[16] X. Xu, Y. Wang, Y. Luo, and D. Hu, "Topology optimization of tensegrity structures considering buckling constraints," Journal of Structural Engineering, vol. 144, no. 10, p. 04018173, 2018.

[17] Y. Kanno, "Topology optimization of tensegrity structures under compliance constraint: a mixed integer linear programming approach," Optimization and Engineering, vol. 14, no. 1, pp. 61-96, 2013.

[18] B. Luo, M.-m. Ding, L.-f. Han, and Z.-x. Guo, "Structural optimization of spoke single-layer cable-net structures based on a genetic algorithm," Journal of Aerospace Engineering, vol. 31, no. 3, p. 04018012, 2018.

[19] E. A. Ahmed, A. O. Nassef, and A. A. El Damatty, "NURBS-based form-finding algorithm for double-curvature cable domes," Journal of Engineering Structures, vol. 283, p. 115877, 2023.

[20] S. Pellegrino, "Structural computations with the singular value decomposition of the equilibrium matrix," International Journal of Solids and Structures, vol. 30, no. 21, pp. 3025-3035, 1993.

[21] E. A. Ahmed, A. O. Nassef, and A. A. El Damatty, "Prestress and size optimization of double-curvature cable domes using an incremental-prestressing iterative technique," Thin-Walled Structures Journal, In press.

[22] Design of steel structures, CAN/CSA-S16-14, Toronto, 2014.

[23] ANSYS Academic Research Mechanical, Release 21.2.

[24] E. Riks, "An incremental approach to the solution of snapping and buckling problems," International journal of solids and structures, vol. 15, no. 7, pp. 529-551, 1979.

[25] S. Krishnan, "Structural design and behavior of prestressed cable domes," Engineering Structures, vol. 209, p. 110294, 2020.